

Complex low-temperature magnetic behaviour of the ordered double-perovskite $\text{Sr}_2\text{RuGdO}_6$

This article has been downloaded from IOPscience. Please scroll down to see the full text article.

2006 J. Phys.: Condens. Matter 18 2273

(<http://iopscience.iop.org/0953-8984/18/7/014>)

View [the table of contents for this issue](#), or go to the [journal homepage](#) for more

Download details:

IP Address: 129.252.86.83

The article was downloaded on 28/05/2010 at 08:59

Please note that [terms and conditions apply](#).

Complex low-temperature magnetic behaviour of the ordered double-perovskite $\text{Sr}_2\text{RuGdO}_6$

Z H Han^{1,4}, H E Mohottala¹, J I Budnick¹, W A Hines¹, P W Klamut^{2,3},
B Dabrowski^{2,3} and M Maxwell³

¹ Department of Physics and Institute of Materials Science, University of Connecticut, Storrs, CT 06269, USA

² Materials Science Division, Argonne National Laboratory, Argonne, IL 60439, USA

³ Department of Physics, Northern Illinois University, DeKalb, IL 60115, USA

E-mail: zhan@phys.uconn.edu

Received 4 October 2005, in final form 22 December 2005

Published 3 February 2006

Online at stacks.iop.org/JPhysCM/18/2273

Abstract

In order to investigate the various interactions in a system consisting of both a 4d transition metal (Ru) and a 4f rare earth (Gd), a combined nuclear magnetic resonance (NMR) and magnetization study has been carried out on the ordered double-perovskite $\text{Sr}_2\text{RuGdO}_6$. As the temperature is reduced, an antiferromagnetic ordering (type-I) of the Ru sublattice occurs at $T_1 = 33$ K, which is a consequence of the Ru–O–O–Ru superexchange interactions. A second magnetic transition occurs between 30 and 10 K, which is characterized by a maximum in magnetization at $T_2 = 17$ K, along with hysteretic behaviour, and reflects the importance of the Ru–O–Gd interactions over this temperature range. For $T_3 < 2$ K, the Gd sublattice orders antiferromagnetically, which is a consequence of the emergence of strong Gd–O–O–Gd interactions. In an external magnetic field, a temperature-dependent spin reorientation is observed. The NMR spectrum for $\text{Sr}_2\text{RuGdO}_6$ at 1.3 K consists of two peaks at 119 and 133 MHz corresponding to the ^{99}Ru and ^{101}Ru isotopes, respectively, and a hyperfine field of 605 kOe. The evolution of the ^{101}Ru NMR peak in an applied magnetic field reveals the existence of a ferromagnetic phase in the antiferromagnetic matrix at low temperature, indicating a complex competition and coexistence of different magnetic interactions in $\text{Sr}_2\text{RuGdO}_6$.

1. Introduction

4d transition metal oxide ruthenates have attracted a great deal of recent interest due to their rich electronic and magnetic properties (for a review, see [1]). In the layered series $(\text{Sr}, \text{Ca})_{n+1}\text{Ru}_n\text{O}_{3n+1}$ (the so-called Ruddlesden–Popper series), these properties range from paramagnetism (CaRuO_3) to antiferromagnetism (Ca_2RuO_4), and from ferromagnetism

⁴ Author to whom any correspondence should be addressed.

(SrRuO_3) to superconductivity (Sr_2RuO_4). The sensitive dependence of these properties on subtle structural changes points to the fact that the 4d orbitals are more extended than 3d orbitals and to the crucial role played by the lattice degrees of freedom. The double-perovskite $\text{Sr}_2\text{RuREO}_6$ (RE = rare earth) compounds are derived from the well-studied perovskite SrRuO_3 , with every other Ru replaced by an RE atom, forming an 'ordered' structure. Despite its structural and electronic proximity to SrRuO_3 , the magnetic ground state of $\text{Sr}_2\text{RuREO}_6$, which is an insulating antiferromagnet (AFM), differs greatly from the itinerant ferromagnetism (FM) found in SrRuO_3 . Band structure calculations on Sr_2RuYO_6 ($Y \neq$ rare earth and does not contribute to the magnetic order) reveal a small energy difference (0.095 eV/Ru) between the FM and the AFM ordering [2], hinting at a strong competition between these two ground states [3].

In a series of earlier works by Battle *et al* [4–8], neutron diffraction was used to study the magnetic structure of the ruthenium double-perovskite $(\text{Ca}, \text{Sr}, \text{Ba})_2\text{Ru}(\text{RE}, \text{Y}, \text{La})\text{O}_6$. In almost all cases, the Ru sublattice adopts a type-I AFM structure at low temperature. The type-I structure consists of moments which are coupled ferromagnetically in the (001) planes; the planes are coupled antiferromagnetically along the [001] direction (or *c*-axis). The only exception that was found is $\text{Ba}_2\text{RuLaO}_6$, which has the type-IIIa AFM structure. In the early neutron diffraction work, the deduced Ru ordered moment was $\approx 2 \mu_B$, which is less than the $3.0 \mu_B$ expected with the t_{2g}^3 electronic structure in the high spin configuration [4–8]. Battle *et al* [4–8] have suggested that the Ru–O–Ru superexchange coupling is mainly responsible for the long range magnetic order. The Ru–RE and RE–RE interactions do not appear to play a significant role except in the case of $\text{Sr}_2\text{RuErO}_6$, where the long range order involves both Ru and Er. The participation of the rare earth elements in the magnetic ordering offers a good opportunity to study the magnetic coupling between the 4d and 4f electron systems, which, presumably, are itinerant and localized, respectively. Gd^{3+} , which possesses a large magnetic moment, might be expected to participate in the magnetic ordering. However, $\text{Sr}_2\text{RuGdO}_6$ was not included in the neutron studies by Battle *et al* [4–8], probably due to the large nuclear absorption cross section of Gd. Papageorgiou *et al* [9] have presented some magnetic work on $\text{Sr}_2\text{RuGdO}_6$ since it is a precursor phase to the extensively studied magnetic superconductor $\text{RuSr}_2\text{GdCu}_2\text{O}_8$. In order to obtain a complete understanding of the magnetic structure and interactions in the $\text{Sr}_2\text{RuGdO}_6$ system, detailed NMR and magnetization studies have been carried out and are reported here.

2. Sample preparation and experimental procedure

A polycrystalline sample of $\text{Sr}_2\text{RuGdO}_6$ (along with a polycrystalline sample of Sr_2RuYO_6 , which was used as a reference sample) was prepared using a conventional solid state reaction technique. A stoichiometric combination of SrCO_3 , RuO_2 , and Gd_2O_3 (Y_2O_3) starting powders were thoroughly mixed, calcined at 950 °C for 12 h in air, ground, and recalcined. The resulting powder was ground again, pressed into a pellet, and sintered at 1380 °C for 36 h under a flowing atmosphere of 70% O_2 and 30% Ar. During the weighing of the RuO_2 starting powder, careful attention was paid to its hygroscopic nature. The final sample powder was characterized by x-ray diffraction using a commercial Bruker powder diffractometer. The diffraction pattern could be entirely indexed using the distorted perovskite-type crystal structure, which is monoclinic with space group $P2_1/n$, and lattice parameters which are consistent with earlier work [10, 11]. Within the sensitivity limits of the instrumentation ($\leq 3\%$), there was no evidence of impurity phases.

The magnetization measurements were carried out on a Quantum Design MPMS SQUID magnetometer operating between 2 and 350 K, and for magnetic fields ranging from –50 to

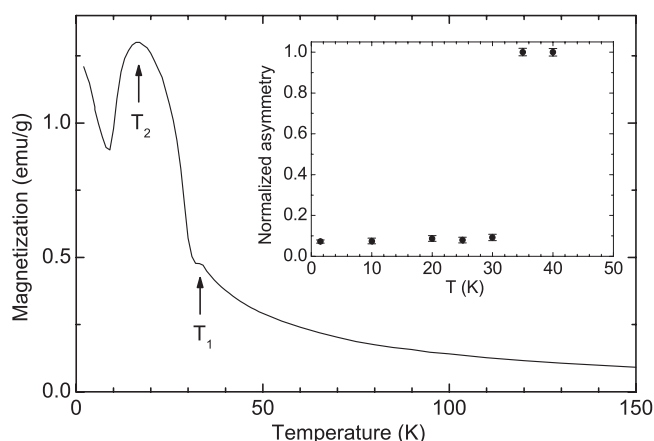


Figure 1. Temperature dependence of the magnetization in 1.0 kOe upon cooling for $\text{Sr}_2\text{RuGdO}_6$. Three consecutive AFM transitions occur at $T_1 = 33$ K, $T_2 = 17$ K (indicated by arrows), and $T_3 < 2$ K, which are attributed to the Ru–Ru, Ru–Gd, and Gd–Gd coupling, respectively. The inset shows the temperature dependence of the muon asymmetry deduced from WTF- μ SR experiments. The magnetic transition at 33 K, which is a consequence of the type-I AFM ordering of the Ru sublattice, is supported by the μ SR experiments.

50 kOe. In the temperature-dependent magnetization measurements, no anomaly was found at 160 K, indicating that the sample is essentially free of SrRuO_3 , an impurity phase which frequently occurs in polycrystalline samples involving both Sr and Ru. Weak transverse field (WTF) muon spin rotation (μ SR) experiments were performed in a field of 100 Oe at the Paul Scherrer Institute (PSI). Spin-echo NMR experiments were carried out at 1.3 K for applied magnetic fields ranging from 0 to 9.0 kOe using a conventional phase-coherent pulse spectrometer. Formation of the spin-echo involved variation of the excitation conditions using a $\pi/2-\tau-\pi$ pulse sequence. The NMR spectra were obtained over the desired frequency range by averaging the spin-echo signal 500–2000 times at various frequencies.

3. Experimental results and analysis

Measurements of the zero-field-cooled (ZFC) and field-cooled (FC) dc magnetization were made for both low (50 Oe) and high (1.0 kOe) magnetic fields. As an example, figure 1 shows the FC magnetization in a field of $H = 1.0$ kOe. As the temperature is reduced, $\text{Sr}_2\text{RuGdO}_6$ undergoes three distinct magnetic transitions at $T_1 = 33$ K, $T_2 = 17$ K, and $T_3 < 2$ K (T_1 and T_2 are marked by the arrows in figure 1). The peak-like features are characteristic of AFM ordering. WTF μ SR data [12] were fitted to Gaussian functions and the asymmetry values at various temperatures were obtained. The temperature dependence of the normalized asymmetry is shown in the inset of figure 1. Since the asymmetry is proportional to the magnetic volume fraction of the system, the magnetic transition at 33 K is supported by the μ SR data. This transition (33 K) is attributed to the type-I AFM ordering of the Ru sublattice via the superexchange path Ru–O–O–Ru. This conclusion is consistent with similar observations in other Ru double-perovskites where the RE ion is diamagnetic; for example, $T_N = 32$ K for both $\text{Sr}_2\text{RuEuO}_6$ and $\text{Sr}_2\text{RuLuO}_6$ [10]. The second magnetic transition, which is characterized by a maximum in the magnetization at 17 K, involves the appearance of weak FM at 30 K with hysteretic behaviour (see below), followed by its disappearance at 10 K. This particular magnetic feature has not yet been reported for other Ru-based double-perovskites, reflecting

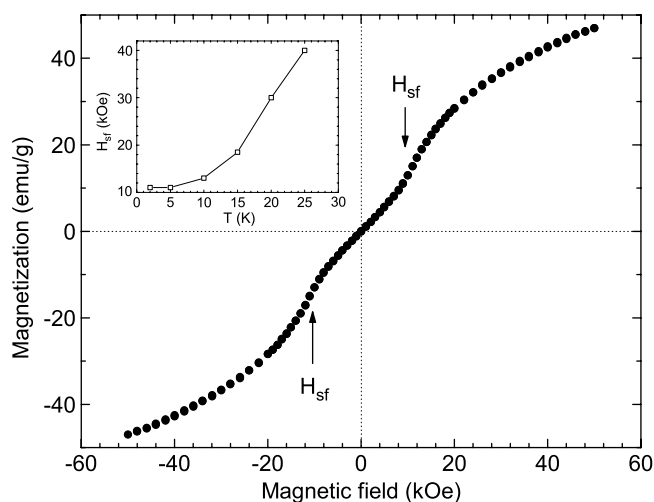


Figure 2. Complete magnetization loop ($-50 \text{ kOe} \leq H \leq 50 \text{ kOe}$) at 5 K for $\text{Sr}_2\text{RuGdO}_6$. No irreversibility is seen, which is consistent with AFM ordering. A spin reorientation (or spin-flop) occurs at a characteristic field H_{sf} (indicated by arrows). The inset shows the temperature dependence of H_{sf} .

the importance of 4d–4f (Ru–O–Gd) magnetic coupling in $\text{Sr}_2\text{RuGdO}_6$. (As discussed below, the weak FM observed here for $\text{Sr}_2\text{RuGdO}_6$ is attributed to a polarization effect of the Gd moments. To date, the observed weak FM in other Ru-based double perovskites, for example, Sr_2RuYO_6 (see [3]), accompanies the AFM order of the Ru sublattice and is not a distinct magnetic transition. Furthermore, the occurrence of the maximum in the magnetization of $\text{Sr}_2\text{RuGdO}_6$ at 17 K reported here and Cao *et al*'s [3] Mott-like transition in the resistivity of Sr_2YGdO_6 at 17 K is strictly a coincidence.) Finally, as the temperature goes below 10 K, a sharp increase in the magnetization occurs; however, this increase deviates from the Curie–Weiss form in that the magnetization appears to bend down below 5 K. This behaviour indicates the onset of a third magnetic transition. Previously, Papageorgiou *et al* [9] reported a cusp near 3 K in one of their $\text{Sr}_2\text{RuGdO}_6$ samples, which apparently depends on the synthesis conditions. This low ordering temperature is reminiscent of $\text{GdBa}_2\text{Cu}_3\text{O}_7$ [13] and $\text{RuSr}_2\text{GdCu}_2\text{O}_8$ [14]. In both systems, neutron diffraction shows that the Gd sublattice undergoes an AFM transition at 2.22 and 2.50 K, respectively. Thus, the Gd sublattice is believed to order at $T_3 < 2 \text{ K}$ in $\text{Sr}_2\text{RuGdO}_6$, independent of the Ru sublattice.

Figure 2 shows the complete magnetization loop ($-50 \text{ kOe} \leq H \leq 50 \text{ kOe}$) measured at 5 K for $\text{Sr}_2\text{RuGdO}_6$. The absence of hysteresis (i.e., no detectable coercive field or remanent magnetization) is consistent with the AFM ordering at this temperature. The magnetization increases linearly with field up to $\approx 10 \text{ kOe}$ where a clear increase in the slope takes place due to a spin reorientation (spin-flop). Observation of a spin-flop indicates the existence of magnetic anisotropy; however, this spin-flop is not believed to be associated with the Gd moments since a sizable magnetocrystalline anisotropy is not expected for Gd sublattice due to a lack of spin–orbit coupling (for Gd^{3+} , $L = 0$). Such a spin-flop was not observed in Sr_2RuYO_6 [3]. Due to the polycrystalline nature of the sample, the expected sudden increase in the magnetization (accompanying the spin-flop) is somewhat broadened. Nevertheless, for $\text{Sr}_2\text{RuGdO}_6$ at 5 K, the ‘critical field’ H_{sf} , which is defined as the field for which the fastest change in the magnetization (coinciding with a local maximum in dM/dH) occurs, is determined to be 11 kOe, as marked

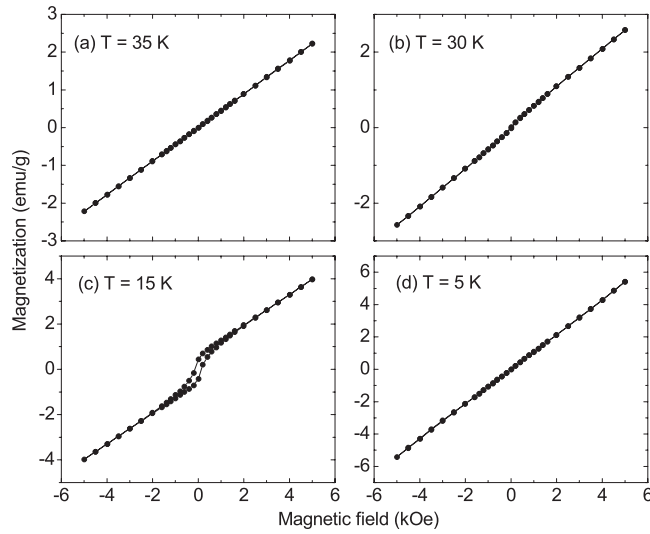


Figure 3. Representative magnetization loops at selected temperatures (with expanded scale for the magnetic field axis) for Sr₂RuGdO₆. Weak FM behaviour is observed for $10 \text{ K} \leq T \leq 30 \text{ K}$, i.e., the region associated with the magnetic transition at 17 K (see figure 1).

by the arrows in figure 2. A careful look reveals that H_{sf} increases with increasing temperature (see the inset in figure 2). The observed temperature dependence can be understood according to

$$H_{\text{sf}} = \sqrt{2K/(\chi_{\perp} - \chi_{\parallel})}, \quad (1)$$

where K is the anisotropy energy [15]. The derivation of above expression involves the minimization of the energy in a field. As can be seen, when the temperature approaches the ordering (Néel) temperature from below, the difference between χ_{\perp} (perpendicular susceptibility) and χ_{\parallel} (parallel susceptibility) approaches zero, and the critical field increases.

Figure 3 shows a representative selection of the magnetization loops (with expanded scale for the magnetic field axis) which were obtained at various temperatures for Sr₂RuGdO₆. Weak FM, characterized by nonlinear or hysteretic behaviour, is just starting to appear for $T = 30 \text{ K}$ (figure 3(b)) and is clearly visible for $T = 15 \text{ K}$ (figure 3(c)). On the other hand, the magnetization loops for $T = 35$ and 5 K (figures 3(a) and (d), respectively) were completely reversible and linear through the origin, indicating no trace of FM behaviour. From all of the magnetization data, it was determined that the weak FM only occurred for $10 \text{ K} \leq T \leq 30 \text{ K}$, i.e., the region corresponding to the large ‘hump’ with a magnetization maximum at 17 K in figure 1. In particular, it should be noted that no trace of nonlinear or hysteretic behaviour was observed at 2 K (a temperature at which both the Gd and Ru moments are ordered), indicating that a simple AFM is associated with both sublattices. The shape of the FC magnetization curve at 1 kOe for $10 \text{ K} \leq T \leq 30 \text{ K}$ (figure 1) reflects the evolution of the weak FM as can be seen by comparing figures 1 and 3. For example, by extrapolating the linear portion of the magnetization versus magnetic field curve (below H_{sf}) at 15 K (figure 3(c)) to zero field, one obtains 0.60 emu g^{-1} for the saturation (spontaneous) magnetization, or $0.057 \mu_{\text{B}}$ per formula unit. Similarly, values for the saturation magnetization can be obtained for other temperatures over this range. As discussed below, this small value which characterizes the weak FM in Sr₂RuGdO₆ is consistent with a polarization of the Gd moments.

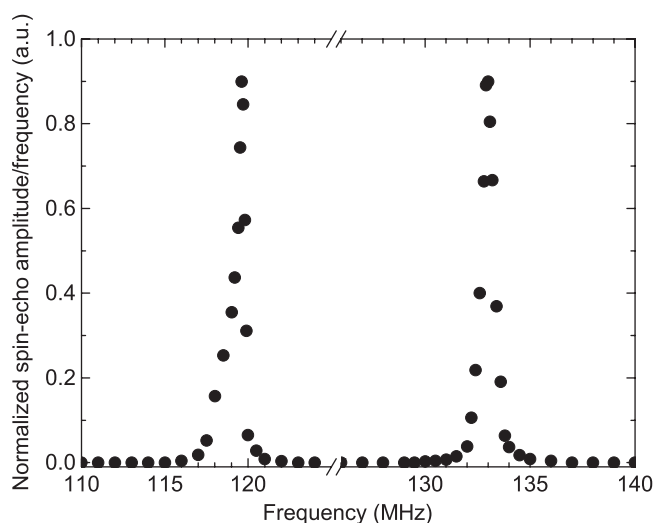


Figure 4. Zero-field spin-echo NMR at 1.3 K for $\text{Sr}_2\text{RuGdO}_6$. The two peaks at 119 and 133 MHz are assigned to the ^{99}Ru and ^{101}Ru isotopes, respectively, and yield a hyperfine field of 605 kOe. An ordered Ru moment of $\approx 2 \mu_B$ is deduced from the peak frequencies.

Concerning the Ru valence and magnetic moment in $\text{Sr}_2\text{RuGdO}_6$, charge neutrality requires Ru to be in the Ru^{5+} state (or $4d^3$ configuration), with half-filled t_{2g} orbitals and empty e_g orbitals in an octahedral crystal field. This results in a spin $S = 3/2$ according to the Hund's rules. Assuming complete orbital quenching, values of $3.0 \mu_B$ and $3.87 \mu_B$ are expected for the Ru ordered moment and paramagnetic moment, respectively. NMR, being a local probe, is a very powerful tool for exploring the Ru valence state and magnetic moment in $\text{Sr}_2\text{RuGdO}_6$.

Figure 4 shows the NMR spectrum obtained for $\text{Sr}_2\text{RuGdO}_6$ at 1.3 K in zero external field. The excitation conditions were independently optimized for the two frequency ranges, namely, 110–125 and 125–140 MHz. It should be noted that, due to the lack of a rf enhancement in an AFM system, low temperatures and high power were required. The NMR spectrum consists of two peaks at 119 and 133 MHz, assigned to the ^{99}Ru (gyromagnetic ratio $\gamma = 0.19645 \text{ MHz kOe}^{-1}$, nuclear spin $I = 5/2$, natural abundance = 12.72%) and ^{101}Ru ($\gamma = 0.22018 \text{ MHz kOe}^{-1}$, $I = 5/2$, natural abundance = 17.07%) isotopes, respectively. These NMR peak frequencies correspond to a hyperfine field of 605 kOe at the Ru nuclei. Taking the widely used (isotropic) hyperfine coupling constant $A \approx 300 \text{ kOe}/\mu_B$ for Ru [16], a value of $\approx 2 \mu_B$ for the local Ru moment is obtained. This value is in good agreement with the ordered Ru moment determined by neutron diffraction for several other Ru double-perovskite systems [4–8]. The reduction (33% compared with the Hund's rule value of $3.0 \mu_B$) indicates a certain degree of itinerancy or covalency through the hybridization of the Ru 4d and O 2p orbitals. In the well-studied itinerant FM SrRuO_3 , where Ru is in the Ru^{4+} state with $S = 1$ ($4d^4$ with low spin configuration), NMR revealed a value of $\approx 1.1 \mu_B$ for the ordered Ru moment, which is a reduction of 45% [17]. Thus, it is concluded that the Ru t_{2g} electrons are more localized in $\text{Sr}_2\text{RuGdO}_6$ than in SrRuO_3 , consistent with the fact that the Ru double-perovskite is categorized as an insulator.

In order to obtain additional magnetic moment information for $\text{Sr}_2\text{RuGdO}_6$, a Curie–Weiss fit was made to the magnetic susceptibility temperature dependence in the paramagnetic state. Such an analysis for $\text{Sr}_2\text{RuGdO}_6$ is complicated by the existence of the two magnetic ions, Ru^{5+} and Gd^{3+} . In an earlier work, Doi *et al* [10] reported that the magnetic contribution from

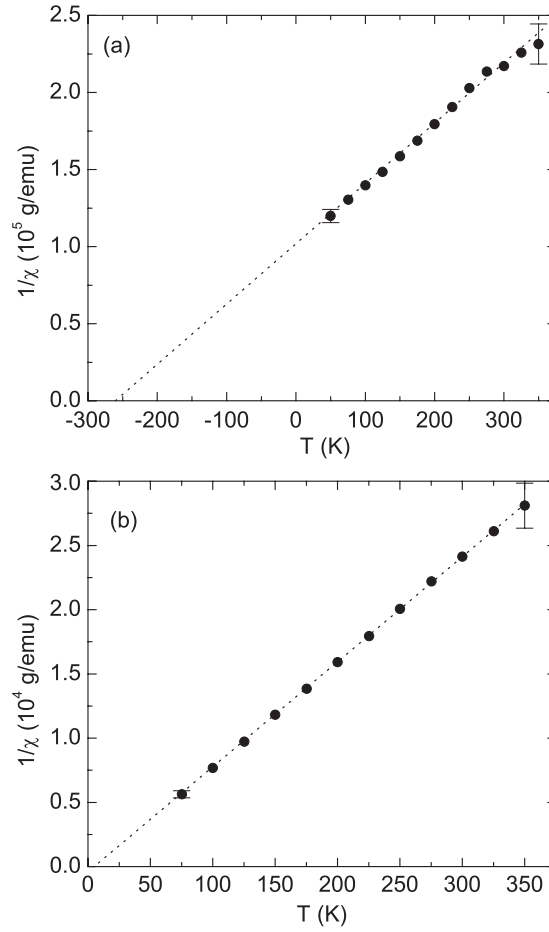


Figure 5. Curie–Weiss fits: (a) for the Ru sublattice contribution in Sr₂RuYO₆ and (b) for the Gd sublattice contribution in Sr₂RuGdO₆. Values of $\mu_{\text{eff}}(\text{Ru}) = 3.1 \mu_{\text{B}}$ and $\Theta(\text{Ru}) = -260 \text{ K}$ obtained from (a) were used to correct for the Ru sublattice contribution in Sr₂RuGdO₆ yielding values of $\mu_{\text{eff}}(\text{Gd}) = 7.2 \mu_{\text{B}}$ and $\Theta(\text{Gd}) = 6.1 \text{ K}$ for the Gd sublattice contribution (b).

the Ru sublattice is ‘negligible’ in the Sr₂RuREO₆ systems for which the RE ions are magnetic. In order to obtain the paramagnetic contribution from the Ru moments, Sr₂RuYO₆ was used as a reference sample, since Y³⁺ has essentially zero magnetic moment. For both the Sr₂RuYO₆ and Sr₂RuGdO₆ samples, meaningful values for the paramagnetic susceptibility $\chi(T)$ were obtained at several temperatures $75 \text{ K} \leq T \leq 350 \text{ K}$ by ensuring that the magnetization versus magnetic field curves were completely linear through the origin and, only then, taking the slope. The susceptibility temperature dependence for Sr₂RuYO₆ was fitted to the Curie–Weiss form

$$\chi(T) = \frac{n\mu_{\text{eff}}^2}{3k_{\text{B}}(T - \Theta)} + \chi_0, \quad (2)$$

where n is the concentration of moments (per g), μ_{eff} is the effective moment (magnitude), k_{B} is the Boltzmann constant, Θ is the Curie–Weiss temperature, and χ_0 is a temperature-independent term which reflects the core diamagnetism, Landau diamagnetism, and Pauli paramagnetism. This resulted in values of $\mu_{\text{eff}}(\text{Ru}) = 3.1 \mu_{\text{B}}$ and $\Theta(\text{Ru}) = -260 \text{ K}$ (see figure 5(a)). From these values, the Ru sublattice contribution in Sr₂RuGdO₆ was then

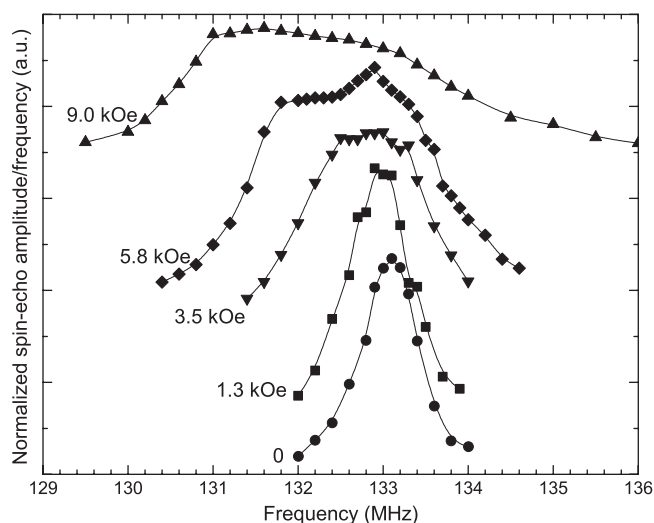


Figure 6. Spin-echo NMR (^{101}Ru peak) with various applied magnetic fields at 1.3 K for $\text{Sr}_2\text{RuGdO}_6$. A peak still remains at 133 MHz while a new peak gradually develops on the low frequency side and shifts down in frequency with increasing field. The new peak arises from a 'ferromagnetic' phase, indicating the existence of different magnetic interactions at low temperature (see text).

calculated using the first term on the right-hand side of equation (2). (It should be noted that the moment concentration (per g) will not be the same for the two systems.) After subtracting the Ru sublattice contribution, a Curie–Weiss fit for the Gd contribution in $\text{Sr}_2\text{RuGdO}_6$ was made. From the fit, values of $\mu_{\text{eff}}(\text{Gd}) = 7.2 \mu_{\text{B}}$ and $\Theta(\text{Gd}) = 6.1 \text{ K}$ were obtained (see figure 5(b)). The Gd^{3+} free-ion moment value is $7.94 \mu_{\text{B}}$. The $\Theta(\text{Gd})$ -value obtained here is very small, as expected, and quite sensitive to the fit which is made at high temperature.

Figure 6 displays the evolution at 1.3 K of the ^{101}Ru NMR peak with increasing magnetic field applied perpendicular to the rf field. For clarity, the spectra are shifted vertically. It can be seen that, in addition to the original peak located at 133 MHz which broadens somewhat with essentially no shift in frequency, a new peak gradually develops on the low frequency side, which shifts to lower frequency with increasing field. Since the applied field makes random angles with the crystallites for a polycrystalline AFM sample, the observed behaviour for the original peak at 133 MHz characterizes the AFM structure of the Ru sublattice [18]. The new peak, on the other hand, indicates the existence of an FM phase (on the timescale of NMR $\sim 10^{-8}$ s) in the AFM matrix. A careful look at the new peak reveals that the shift in frequency is a linear function of the applied field with a slope of $-0.23 \text{ MHz kOe}^{-1}$ (see figure 7). This value is very close to the gyromagnetic ratio for the ^{101}Ru isotope ($0.22018 \text{ MHz kOe}^{-1}$), indicating that this FM phase can be very easily saturated. Since the saturated FM phase is fully aligned by the external field, the frequency shift would follow the gyromagnetic ratio. The negative shift demonstrates that the hyperfine field is predominantly due to the core polarization mechanism, i.e., the hyperfine field is opposite in direction to the magnetization. It should be pointed out that this FM phase (at 1.3 K) cannot be interpreted as the canting of the AFM sublattice, for which a much smaller shift is expected. Furthermore, the lack of hysteresis at 2 K strongly suggests that this phase is single domain in nature, which behaves superparamagnetically under the macroscopic SQUID measurement. The application of an external field suppresses the superparamagnetic relaxation, causing more domains to exhibit ferromagnetic behaviour

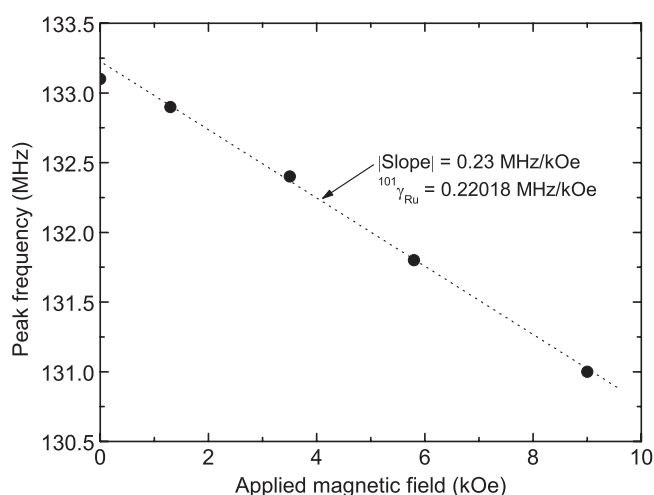


Figure 7. Field dependence of the new low-frequency ¹⁰¹Ru NMR peak (from figure 6) at 1.3 K for Sr₂RuGdO₆.

and, therefore, enhances the NMR intensity [19]. Consequently, the new peak becomes more pronounced with increasing field. An accurate determination of the volume fraction of the FM phase is not possible from the NMR intensities, since different enhancement factors are associated with the two magnetic phases.

4. Discussion and conclusions

As the temperature is reduced, three consecutive and distinct magnetic transitions are observed for Sr₂RuGdO₆ at $T_1 = 33$ K, $T_2 = 17$ K, and $T_3 < 2$ K. Weak FM appears at 30 K and then disappears at 10 K. The appearance and subsequent disappearance of weak FM, along with successive magnetic transitions, has not been reported for other Ru–RE double-perovskite systems to date. In addition, a spin reorientation (or spin-flop) is observed for Sr₂RuGdO₆. These observations illustrate the roles played by the various interactions in a system consisting of both a 4d transition metal (Ru) and a 4f rare earth (Gd).

As in Sr₂RuErO₆ [8], the magnetic order in Sr₂RuGdO₆ involves both Ru and the RE constituent (Gd). Unlike the 4d electrons for Ru, the 4f electrons for Gd are presumably localized, which does not favour overlap with the O p orbitals. Thus, the magnetic coupling involving Gd is quite unique. The possible superexchange interactions in Sr₂RuGdO₆, in order of expected strength, are: (1) Ru–O–O–Ru (Ru–Ru hereafter), (2) Ru–O–Gd (Ru–Gd hereafter), and (3) Gd–O–O–Gd (Gd–Gd hereafter) [8].

As in other Ru double-perovskites, the Ru–Ru interaction initiates the transition at $T_1 = 33$ K, below which the system enters a type-I AFM state due to the magnetic order of the Ru sublattice [4–8]. Due to its lower energy, the AFM ordering is favoured over a FM ordering and, as a result, an insulating gap opens up between the majority and the minority spin states [2]. The Ru–Gd interaction becomes significant upon cooling and results in a second magnetic transition which is characterized by a maximum in the magnetization at 17 K (see figure 1), along with weak FM behaviour for $10 \text{ K} \leq T \leq 30 \text{ K}$ (see figure 3). The emergence of strong Gd–Gd coupling at low temperature results in an ‘independent’ magnetic ordering of the Gd sublattice below 2 K. This is typical of the ordering temperatures due to the Gd–Gd interaction

in other perovskite systems [13, 14]. Gd is believed to adopt a magnetic structure similar to that of Ru in $\text{Sr}_2\text{RuGdO}_6$, as is the case for Er in $\text{Sr}_2\text{RuErO}_6$ [8]. No irreversibility in the $M-H$ curve is seen at 2 K, indicating that no FM component exists in either the Gd or Ru sublattice.

In an earlier work, the weak FM that occurs for $10 \text{ K} \leq T \leq 30 \text{ K}$ was attributed to the polarization effect of the Gd moments due to the canting of the Ru sublattice [9]. However, the complete absence of FM at both 2 and 5 K (see figure 3(d)) makes this scenario somewhat unlikely. Any canting of Ru moments which occurs at $\approx 30 \text{ K}$ would then have to disappear by 5 K without any other mechanism, e.g., structural phase transition, being reported. Another possible explanation is that the magnetoelastic stress which is placed on the lattice due to the AFM ordering of the Ru sublattice leads to a very small crystallographic distortion. This breaks the crystal symmetry of the Ru moments resulting in an internal field which polarizes the Gd moments. This second scenario, which does not require a canting of the Ru moments, was proposed in a detailed magnetic study of Gd_2CuO_4 single crystals carried out by Thompson *et al* [20]. As is the case with compounds of the RE_2CuO_4 family, Gd_2CuO_4 exists in a tetragonal crystal structure that contains CuO_2 planes perpendicular to the c -axis, with the oxygen atoms being square-planar coordinated about the copper atoms. The Cu sublattice undergoes an AFM ordering in these planes at 260 K. As the temperature is reduced, a weak FM appears, and subsequently disappears, with a maximum at 20 K. Finally, the Gd sublattice undergoes an AFM ordering at 6.5 K. The weak FM behaviour observed by Thompson *et al* [20] for Gd_2CuO_4 , which is completely analogous to that observed here for $\text{Sr}_2\text{RuGdO}_6$, is characterized by a saturation magnetization having the comparable value of $0.052 \mu_{\text{B}}$ per formula unit at the 20 K maximum. In $\text{Sr}_2\text{RuGdO}_6$, the oxygen atoms are octahedrally coordinated about the ruthenium atoms. The Ru (and Gd) moments also order antiferromagnetically in planes perpendicular to the c -axis. The polarizing effect is expected to disappear after the Gd sublattice is completely ordered (AFM).

Another good example of a system where the Gd sublattice is polarized through its interaction with the Ru sublattice is the well-known magnetic superconductor $\text{RuSr}_2\text{GdCu}_2\text{O}_8$. Detailed magnetization and polarized neutron diffraction studies clearly show (a) an AFM ordering of the Ru sublattice at $\approx 136 \text{ K}$, (b) weak FM which includes the polarized Gd moments [14, 21]. A value of $\approx 0.1 \mu_{\text{B}}$ per formula unit is obtained for the weak FM component, which is completely consistent with the results for both Sr_2RuGd_6 in this study and Thompson *et al*'s [20] Gd_2CuO_4 .

It should be noted that the (Gd) polarization mechanism described above is different from that proposed to account for the weak FM in Sr_2RuYO_6 [3], where either a canting of the Ru moments or the antisymmetric Dzyaloshinskii–Moriya interaction was suggested. In Sr_2RuYO_6 , the weak FM behaviour remains down to the lowest measurement temperature at 5 K [3]. In contrast, the weak FM in $\text{Sr}_2\text{RuGdO}_6$ reported here disappears at low temperature due to the AFM ordering of the Gd sublattice.

Battle *et al* [8], in analysing $\text{Sr}_2\text{RuErO}_6$, conclude that the apparent type-I order of the Er sublattice is an inevitable consequence of the Ru–Ru and Ru–Er coupling, rather than direct Er–Er interaction. As a result, the true magnetic structure is more accurately described as C-type, provided that the difference between the two moments is ignored. The existence of three transitions in $\text{Sr}_2\text{RuGdO}_6$ indicates that the magnetic order of the Gd sublattice due to the direct Gd–Gd interaction is rather independent of the Ru sublattice order. This is a result of the more extended 4f orbitals in Gd than in Er. As a consequence, magnetic order of the Er sublattice due to the direct Er–Er interaction is expected to occur at lower temperature. This is supported by a study of the rare earth sublattice ordering in $\text{REBa}_2\text{Cu}_3\text{O}_x$, where the ordering temperatures were found to be 2.24 and 0.6 K for $\text{GdBa}_2\text{Cu}_3\text{O}_x$ and $\text{ErBa}_2\text{Cu}_3\text{O}_x$, respectively [22]. Since the neutron work on $\text{Sr}_2\text{RuErO}_6$ by Battle *et al* [8] was done at 4.2 K, well above the Er–

Er ordering temperature, a C-type AFM structure is reasonable. In the case of Sr₂RuGdO₆, a strong Gd–Gd interaction prevails at low temperature and a more complicated magnetic structure results which involves interpenetrating type-I AFM of Gd and Ru sublattices.

In conclusion, the magnetic properties and hyperfine interactions in the ordered double-perovskite Sr₂RuGdO₆ have been studied. Magnetization measurements reveal successive magnetic transitions associated with particular superexchange interactions. Spin-echo NMR indicates that Ru is in the Ru⁵⁺ state with rather localized t_{2g} electrons. The local moment and hyperfine field of Ru are determined to be ≈2 μ_B and 605 kOe, respectively. The field-dependent NMR studies reveal that there exist two components characterized by AFM and FM behaviour in Sr₂RuGdO₆, i.e., the magnetic ground state of Sr₂RuGdO₆ at low temperature involves complex coexistence and competition of different interactions. A model is proposed to explain why FM does not appear in the bulk magnetization.

Acknowledgments

The authors would like to acknowledge the Paul Scherrer Institute where the μSR experiments were carried out. The research at UConn was supported by the US-DOE through contract DE-FG02-00ER45801.

References

- [1] Cao G, Alexander C S, McCall S, Crow J E and Guertin R P 1999 *Mater. Sci. Eng. B* **63** 76
- [2] Mazin I I and Singh D J 1997 *Phys. Rev. B* **56** 2556
- [3] Cao G, Xin Y, Alexander C S and Crow J E 2001 *Phys. Rev. B* **63** 184432
- [4] Battle P D, Goodenough J B and Price R 1983 *J. Solid State Chem.* **46** 234
- [5] Battle P D and Macklin W J 1984 *J. Solid State Chem.* **52** 138
- [6] Battle P D and Macklin W J 1984 *J. Solid State Chem.* **54** 245
- [7] Battle P D and Jones C W 1989 *J. Solid State Chem.* **78** 108
- [8] Battle P D, Jones C W and Studer F 1991 *J. Solid State Chem.* **90** 302
- [9] Papageorgiou T P, Herrmannsdörfer T, Dinnebier R, Mai T, Ernst T, Wunschel M and Braun H F 2002 *Physica C* **377** 383
- [10] Doi Y and Hinatsu Y 1999 *J. Phys.: Condens. Matter* **11** 4813
- [11] Greatrex R, Greenwood N N, Lal M and Fernandez I 1979 *J. Solid State Chem.* **30** 137
- [12] Mohottala H E *et al* unpublished
- [13] Paul D McK, Mook H A, Hewat A W, Sales B C, Boatner L A, Thompson J R and Mostoller M 1988 *Phys. Rev. B* **37** 2341
- [14] Lynn J W, Keimer B, Ulrich C, Bernhard C and Tallon J L 2000 *Phys. Rev. B* **61** R14964
- [15] Morrish A H 1980 *The Physical Principles of Magnetism* ed E Robert (Huntington, NY: Krieger) p 475
- [16] Kumagai K, Takada S and Furukawa Y 2001 *Phys. Rev. B* **63** 180509(R)
- [17] Han Z H, Budnick J I, Hines W A, Dabrowski B, Kolesnik S and Maxwell T 2005 *J. Phys.: Condens. Matter* **17** 1193
- [18] Allodi G, De Renzi R, Licci F and Pieper M W 1998 *Phys. Rev. Lett.* **81** 4736
- [19] Zhang Y D, Hines W A, Budnick J I, Zhang Z and Sachtler W M H 1994 *J. Appl. Phys.* **76** 6576
- [20] Thompson J D, Cheong S-W, Brown S E, Fisk Z, Oseroff S B, Tovar M, Vier D C and Schultz S 1989 *Phys. Rev. B* **39** 6660
- [21] Jorgensen J D, Chmaissem O, Shaked H, Short S, Klamut P W, Dabrowski B and Tallon J L 2001 *Phys. Rev. B* **63** 054440
- [22] Brown S E, Thompson J D, Willis J O, Aikin R M, Zirngiebl E, Smith J L, Fisk Z and Schwarz R B 1987 *Phys. Rev. B* **36** 2298